(6 THE EFFECT OF OXYGEN ADDITIONS ON THE PROPERTIES

OF AMORPHOUS TRANSITION METAL ALLOYS

D.E. /Polk, [+][c] C.E. /Dube [*] and B.C. /Giessen [+][a]

+ Institute of Chemical Analysis, Applications and Forensic Science, Northeastern University, Boston, Massachusetts, USA 02115

* Department of Chemistry, Northeastern University, Boston, Massachusetts, USA 02115

1978

Introduction

(2) 11

Oxygen contamination is a potential problem in the study of amorphous metals because of the highly reactive nature of some of the constituent elements of metallic glasses and because of the processing techniques which are used to produce this metastable state. Oxygen is frequently present already in the starting materials, e.g. rare earth elements or early transition metals; further, oxygen present as an impurity in the gaseous atmosphere may be incorporated during alloy preparation (e.g. arc melting) or during the quench process (especially during thermal evaporation or sputtering or during splat quenching using the gun technique). Since these materials are generally studied as thin foils, further heat treating of the amorphous metal can also lead to a significant oxygen contamination. Nitrogen contamination may be a similar problem under these circumstances, but this impurity was not studied at the present time.

Effects of oxygen on the formation of and/or the behavior of amorphous metals have been noted previously. In sputtering or vapor deposition, the presence of oxygen has been shown to enhance the formation of an amorphous structure from unalloyed metals; for example, it has been shown[1,2] that a nickel film deposited by electron-beam evaporation onto a substrate held at 4 K is crystalline when optimum ultra-high vacuum conditions are used while the inclusion of gaseous impurities at a level of ~0.7% leads to an amorphous deposit with a crystallization temperature of ~50 K.[1] Other films of "amorphous Ni" have been reported to crystallize at much higher temperatures, e.g. 530 K,[3] undoubtedly due to higher levels of contamination by, at least in part, oxygen. Oxygen contamination can also readily stabilize the amorphous phase in films prepared by sputtering from a high purity nickel target.[4] Further, a noncrystalline structure was observed in thin, electron transparent regions of nickel foils produced by gun-technique splat quenching of initially unalloyed nickel onto a room temperature substrate;[5] the high T_c = 425 K of this material was attributed to oxygen contamination.[5]

It is clear that the presence of oxygen in amorphous metals can also affect the crystalline phases which form on crystallization as well as the thermal stability of the alloy. It has been observed, for example, that a new crystalline phase (η carbide, W_3Fe_3C type) formed upon heat treating of amorphous Ti-Be alloys in a calorimeter[6] and is found in a Ti-Be-O alloy due to its stabilization by the presence of oxygen and/or nitrogen.[7]

In this study, oxygen has been added to three binary inter-transition metal alloys already known to form a glass upon rapid liquid quenching. The effect of

oxygen upon the glass forming ability, the glass transition behavior, the ductility of the glasses and their crystallization products has been characterized.

Experimental

Alloys were prepared by melting together the pure metals and, for oxygen containing alloys, pressed pellets of copper oxide powder and nickel oxide powder (86 w/o Cu and 75.2 w/o Ni; Alfa Products, Ventron Corporation) in an arc-melting furnace. $Zr._{50}Cu._{50}$, $Nb._{50}Ni._{50}$ and $Ti._{667}Ni._{333}$ were selected as the basic binary alloy compositions to be studied; oxygen additions to these alloys were then made such that the metal ratio was kept constant. Alloys were not analyzed chemically after melting; indicated compositions are those calculated from the initial weights of the components. Rapid liquid quenching was accomplished using an arc-melting hammer and anvil apparatus and also, for the Zr-Cu-O alloys, melt spinning from a fused silica crucible onto the inside of a rotating cup. Standard X-ray diffractometer procedures with filtered $CuK\alpha$ radiation were used for structural characterizations. A Perkin-Elmer DSC2 (with 99.996% argon gas as protective atmosphere) was used for all thermal treatments; data was recorded on a two pen recorder so that the DSC2 output could be gathered at two different sensitivities.

Results and Discussion

Data on glass formation and thermal stability for the alloys which were studied are given in Table 1.

Compositions which form a glass.

For the $Zr._{50-x/2}Cu._{50-x/2}O_x$ alloys, glasses were obtained with up to 8 a/o oxygen by using the arc-melting quench unit; attempts to obtain the amorphous phase for alloys containing $\geq$ 10 a/o oxygen were unsuccessful. Results of the hammer-and-anvil quench process were not fully reproducible from splat to splat; some splats have a higher yield of metallic glass than others since the foil thickness and hence quench rate can vary from splat to splat. This observation can be used to qualitatively judge the relative glass forming ability of different alloys by quenching each composition several times and comparing the results. While binary $Zr._{50}Cu._{50}$ forms a glass readily upon arc quenching, it was found that the addition of oxygen progressively reduces the glass forming ability so that alloys containing 8 a/o and, to a lesser extent, 6 a/o oxygen could be made amorphous only with great difficulty.

$Zr._{50}Cu._{50}$ could be readily melt spun to a glass in vacuum. However, all $Zr._{50-x/2}Cu._{50-x/2}O_x$ alloys, even with only 1 a/o oxygen, were partially crystalline when melt spun under similar conditions. Ribbons from alloys of low oxygen content appeared amorphous on the substrate side but were partly crystalline on the top surface; they exhibited a crystalline pattern superimposed on a broad amorphous peak. This is consistent with our experience that the arc-melting hammer-and-anvil quench method produces higher quench rates than we could achieve by melt spinning. The results from melt spinning are discussed further in the section on crystalline phases.

For $Nb._{50-x/2}Ni._{50-x/2}O_x$, a glass was obtained upon quenching in the arc-melting unit with 2.9 and 5.7 a/o oxygen; alloys containing $\geq$ 8.6 a/o oxygen could not be made fully amorphous.

$Ti._{667}Ni._{333}$ could be quenched to a fully amorphous condition in the arc-melting unit. However, repeated attempts to produce fully amorphous Ti-Ni-O samples containing even only 1 or 2 a/o oxygen by this method were unsuccessful.

Thermal behavior by calorimetry: T_g and T_c.
_____

Fig. 1 illustrates the DSC2 thermograms obtained for the amorphous Zr-Cu-O
samples. Data in Fig. 1 was gathered from samples weighing ∿9 mg at a heating
rate of 80 K/min; one pen, having a full-scale deflection sensitivity of
5 mcal/sec, was appropriate for investigating the glass transition for the
selected mole fraction and heating rate and the 50 mcal/sec sensitivity of the
other pen was selected so that the full crystallization exotherm could be
observed.

It can be seen in Fig. 1 that the $Zr_{.50}Cu_{.50}$ alloy, as observed previ-
ously,[8,9] exhibits a well defined thermal manifestation of the glass transition,
i.e. a ΔC_p, and that the specific heat has "levelled off" at the higher value
associated with the undercooled liquid.[10] The value of ΔC_p observed for
$Zr_{.50}Cu_{.50}$, 4.6 cal/mole K, is typical of that measured for other metallic
glasses where the "levelling off" is seen. The addition of 2 a/o oxygen raises
T_g by 21 K though crystallization now beings sooner, relative to T_g, than in the
oxygen free alloy so that the "levelling off" of C_p at the higher value is
therefore not observed. It appears that, with increasing oxygen content, T_g
moves to higher temperatures faster than T_c, i.e. $(T_c - T_g)$ decreases, such that
only part of the ΔC_p is seen for the 4 a/o oxygen alloy and no ΔC_p is seen for
the 6 and 8 a/o oxygen glasses. In general, a ΔC_p may or may not be seen for
any given oxygen free amorphous metal since $(T_c - T_g)$ varies as the composition
varies.[11]

It had been noted previously[11] that metallic glasses can be prepared more
readily by rapid liquid quenching, i.e. with lower quench rates, as their
$(T_c - T_g)$ increases. Since the atomic mobility increases rapidly for $T > T_g$,[12]
alloys of higher $(T_c - T_g)$ possess relatively higher atomic mobilities before
crystallization occurs; the higher resistance to crystallization near the glass
transition temperature thus appears to extend throughout the entire temperature
range corresponding to the undercooled liquid. Thus, the fact that $(T_c - T_g)$ of
the present alloys decreases as the oxygen content increases is consistent with
the finding noted in the previous section that the ease of glass formation
decreases as oxygen is added.

At temperatures preceding any glass transition and crystallization effects,
all of the samples are seen to exhibit a broad exothermic "relaxation" effect
over a temperature interval of about 200 K; this effect was previously noted for
Pd-Si alloys[13] and for Zr-Cu alloys.[3] In Fig. 1, comparison of the amorphous
curves with the curves taken for the samples after crystallization makes this
effect apparent.

The crystallization exotherm is seen to broaden significantly at oxygen
contents above 2 a/o. As mentioned, the onset temperature moves to higher
temperatures as the oxygen content increases with a maximum increase of T_c of
∿40 K at 6 a/o oxygen before it decreases for the 8 a/o oxygen alloy.

For the interpretation of the present results it is of major importance to
decide whether or not: (1) the oxygen was in fact uniformly distributed through-
out the amorphous phase and (2) the composition of the glass was as calculated
from the initial components, e.g. whether or not oxygen was lost during melting.

As to the first point, the strongest argument that the oxygen is dissolved
uniformly (on a microscopic scale) is the marked and smooth change in the glass
transition behavior as a function of the nominal oxygen content (Fig. 1). We
base an argument for local homogeneity on the reproducibility and compositional
dependence of the thermal features for binary Zr-Cu glasses. We have found the
"shape" of the glass transition for $Zr_{.50}Cu_{.50}$, determined by the relative
temperatures of T_g and the onset of crystallization, to be quite reproducible

for alloys of this composition which were prepared, quenched and characterized on different occasions, using both the arc-quench method and melt spinning. Further, the "shape" of the glass transition is relatively constant in the vicinity of $Zr_{.50}Cu_{.50}$ as the ratio of Zr to Cu is changed.[9] Thus, the observed changes in the glass transition behavior can not be due, e.g., to the segregation of the oxygen into more zirconium rich regions, leaving behind the bulk of the material as a glass richer in copper than the $Zr_{.50}Cu_{.50}$ alloy.

As to the second point, the weight losses occurring upon preparation of the alloys containing oxygen in the arc-melting furnace were typical of the less than 1 w/o loss experienced for nominally oxygen-free alloys. Further, after crystallization the amorphous alloys from the initial pellets containing oxygen contained significant amounts of phases which were different from those found for the nominally pure alloys and which are known to be stabilized by oxygen; this is discussed in more detail in the subsequent section on crystal phases.

Finally, the data are found to be internally consistent with good reproducibility. Different splats of nominally the same composition generally had T_c's within ± 5 K (presumably due to compositional fluctuations between the ~50 mg alloy pieces chipped from the master alloy and then used for arc-quenching) of the average value and had similar glass transition behavior, i.e. the "shape" of the C_p change or the absence of such a change.

T_c values for Nb-Ni alloys are given in Table 1. Upon scanning amorphous $Nb_{.50}Ni_{.50}$ at 80 K/min, no crystallization exotherm was observed below 1000 K, the temperature limit of the DSC2. Upon scanning at 10 K/min, however, a crystallization exotherm was observed; accordingly, the Nb-Ni-O glasses were also run at a heating rate of 10 K/min. For the oxygen-containing alloys, a second peak appeared at lower temperatures; i.e. in contrast to the Zr-Cu alloys, the presence of oxygen caused crystallization to occur at a lower temperature. The first peak accounted for ~38% of the heat of crystallization in the alloy with 2.9 a/o oxygen and ~47% of the heat of crystallization in the alloy with 5.7 a/o oxygen. For a scan rate of 10 K/min and the available amount of sample, it was not possible to determine the C_p behavior of these alloys immediately before crystallization in detail.

Heating rate dependence of crystallization and isothermal annealing.

A more detailed comparison of the crystallization behavior of the binary $Zr_{.50}Cu_{.50}$ glass and a ternary Zr-Cu-O glass was desired. For such studies, melt-spun ribbons would be desirable in order to avoid any small variations possible between nominally identical glasses prepared by arc quenching; this is necessary since experiments for the determination of the activation energy for crystallization involve only small changes in the crystallization temperature. However, the inability to produce fully amorphous melt-spun Zr-Cu-O ribbons hampered this comparison.

Portions of an amorphous $Zr_{.50}Cu_{.50}$ ribbon were scanned at heating rates of 10 K/min to 160 K/min; the qualitative features of the crystallization exotherm did not change. The crystallization temperatures obtained in these runs are given in Table 1. In order to determine the activation energy for crystallization ΔE_c, $\ln T_p/\alpha$ vs. $1/T_p$ was plotted;[14] however, rather than a straight line, a "smooth", curved line was obtained. The tangent to the portion of the curve obtained at low heating rates (10 to 20 K/min) resulted in a value of ΔE_c = 96 Kcal/mole and that for high heating rates (80 to 160 K/min) gave ΔE_c = 75 Kcal/mole. Because the sample may not track the indicated temperatures at the high rates exactly and because of the results of isothermal annealing experiments given below, the value derived from the lower heating rates is preferred.

Isothermal runs, where the rate of evolution of heat as a function of time was measured, were also conducted. As illustrated in Fig. 2, a single peak was observed for $Zr_{.50}Cu_{.50}$. Isothermal data were recorded from 690 K to 715 K at intervals of 5 K. A plot of $\ell n(time)$ (both for times corresponding to the maximum rate of heat evolution and for times corresponding to 1/5 of this maximum rate) vs. $1/T$ gave a straight line with a slope corresponding to a $\Delta E_c = 97$ Kcal/mole for both stages of crystallization, in good agreement with the value quoted above determined from variation of the heating rate.

Since data for oxygen-containing alloys had to be obtained from splats, only the heating rate variation method (which can be done with smaller amounts of sample so that one splat can be used for several runs) was practical, given the small variations between splats of nominally identical composition. Sections of one splat of amorphous $Zr_{.49}Cu_{.49}O_{.02}$ were run at different heating rates. As for $Zr_{.50}Cu_{.50}$, the shape of the crystallization exotherm was unchanged by changes in the heating rate though the exotherms for the 2 a/o oxygen alloy have a distinct shoulder on the low temperature side, unlike that for $Zr_{.50}Cu_{.50}$. The $\Delta E_c = 95$ Kcal/mole calculated from the variation of T_p for the 2 a/o oxygen glass is essentially identical to that found for $Zr_{.50}Cu_{.50}$ though this ΔE_c value is associated with the main peak; the shoulder may be due to the formation of the η phase (see below) which may have a different ΔE_c.

In contrast to the thermal scans, the 2 a/o oxygen alloy behaves markedly different from the $Zr_{.50}Cu_{.50}$ alloy upon isothermal annealing. Fig. 2 also illustrates the thermogram from a 2 a/o oxygen foil annealed at 700 K; while some variation between different samples was observed, these thermograms generally show two peaks. X-ray diffraction measurements of a sample after the first peak show the first peak to be associated with $\sim 20\%$ of the sample forming a microcrystalline η phase (W_3Fe_3C type) (see below). The second peak corresponds to the crystallization of the remaining amorphous phase to α-ZrCu.

The difference in the crystallization behavior of the binary and ternary alloys, including the formation of the η phase (W_3Fe_3C type) which is often stabilized by the presence of oxygen,[15] is a further indication that the oxygen has remained in solution in the alloy.

Crystalline phases.

For $Zr_{.50}Cu_{.50}$, the α-ZrCu phase is found both in the as-cast alloy and after the DSC scan of the initially amorphous sample. For Zr-Cu-O samples, both α-ZrCu and an η phase (W_3Fe_3C type) form in the single exotherm seen in the DSC scan with, as expected, the relative proportion of the η phase increasing as the oxygen content increases.

After crystallization during the DSC scan, the $Nb_{.50}Ni_{.50}$ alloy did not have the hexagonal μ phase structure expected from the phase diagram[15] and present in the alloy before quenching. Instead a more complex XRD pattern was found, the principal lines of which (in the forward reflection region) could be tentatively indexed with an orthorhombic unit cell corresponding to the M phase type found as an equilibrium phase in the Nb-Ni-Al system[16] and other ternary Nb-Ni alloys.[17] The M phase had earlier been observed in an isothermally annealed, splat cooled Nb-Ni glass.[18] Further annealing tests would be required to determine whether the observed M phase is a metastable binary phase or whether it was being stabilized by unknown low-level impurities. In any case, the effect of oxygen additions at levels of ≥ 2 at.pct. is different: for both Nb-Ni alloys which initially contain oxygen, the low temperature exotherm was associated with the formation of a ternary phase, reported earlier as an equilibrium phase,[19] that has the η phase (W_3Fe_3C type) structure and coexists with the remaining amorphous phase; the second exotherm is due to the crystallization of the remaining amorphous material to the M-phase. The relative amounts of η and the amor-

phous phases indicate that, if the oxygen is totally concentrated in the η phase of equal Nb and Ni content, the η phase would have a composition near $Nb_3Ni_3O_x$ with $x \sim 0.5$.

This crystallization behavior of the Nb-Ni-O alloys is similar to the two-step crystallization of $Zr_{.49}Cu_{.49}O_{.02}$ upon isothermal annealing which was discussed previously. Thus, in both systems, segregation takes place during crystallization, with oxygen migrating from the glass to form a metal-rich, oxygen stabilized ternary phase.

As confirmed in this study where $Ti_{.667}Ni_{.333}$ was arc-quenched into a fully amorphous foil, it had been noted previously[23] that a glass could be made at the composition of the intermetallic phase Ti_2Ni. This equilibrium compound has a structure[21] which is closely related to the W_3Fe_3C structure discussed above. For Ti-Ni alloys, however, oxygen additions even as low as 1 a/o resulted in splats which were <u>partly</u> crystalline, suggesting oxygen segregation during the processing, apparently due to additional stabilization of this phase by oxygen.

Fig. 3 shows the diffraction pattern obtained from the crystallized $Zr_{.49}Cu_{.49}O_{.02}$ foils superimposed on the broad first peak characteristic of the glass. The two main peaks at $\sim 37°$ and $\sim 40°$ are from α-ZrCu (though the intensity of the peak at $\sim 37°$ would be relatively higher in a non-textured sample); the peak between them is at the position of the main peak of the η phase (W_3Fe_3C type) in the Zr-Cu-O alloys; while there is overlap with a peak from α-ZrCu and possibly β-ZrCu at the same location, it may indicate the presence of the η phase even in the 2 a/o oxygen alloy.

In general, the major diffraction peaks for any intermetallic phase having a composition near that of the glass, as well as the first reflection of a hypothetical fcc or bcc structure of appropriate atomic volume, occur near the center of the broad peak. As seen in Fig. 3, this is the case for a fcc $Zr_{.5}Cu_{.5}$ structure which maintains the elemental atomic volumes; it is also the case for the α-ZrCu and the closely related Zr_7Cu_{10} structure as well as the oxygen stabilized η phase which has been found here in the ternary system.

In contrast, the major peaks of the ZrO_2 phases are found at much larger d values and lower 2θ, as indicated in Fig. 3. The peak seen at 2θ of $\sim 28°$ in the crystalline pattern from $Zr_{.49}Cu_{.49}O_{.02}$ is in fact due to monoclinic ZrO_2. The atmosphere in the DSC2 was not sufficiently clean to prevent some oxidation of the sample during the runs, and some "blackening" of the surface is generally visible to the eye. After longer annealing times and/or higher temperatures, the ZrO_2 lines become more intense, including the well defined, second most intense reflection of monoclinic ZrO_2 and a reflection from tetragonal ZrO_2. In each case, these lines ascribed to ZrO_2 disappear upon a light polishing of the surface of the annealed sample.

In analogy with other inorganic oxide glass systems (e.g. the SiO_2 system[22]), it is expected that the broad first peak of an amorphous phase having short range order similar to that in monoclinic ZrO_2 would occur at about $28°$. This statement is of interest since broad peaks at about this location have been observed in previous studies of Zr-Cu alloys.[23,24] In a transmission electron microscopy study[23] of foils heat treated so as to initiate crystallization, regions within the foil which were associated with a broad halo at k values corresponding approximately to the crystalline peak of ZrO_2 mentioned above were found. This phase was labelled the "transformed amorphous phase" and was generally found at the boundary between growing crystals and the amorphous matrix.[23] In view of the small relative difference in the scattering powers of Zr and the Cu, it is not considered possible that an amorphous (or crystalline) structure based only on Cu and Zr would have significant values of the interference function (or structure factor) at the observed low k values, i.e. that it would have a halo

at such a low angel. Even amorphous pure Zr would presumably have a broad peak centered at an angle not lower than $\sim 34°$. Thus, it is suggested that the "transformed amorphous" material is likely to be rich in oxygen, formed either by the expulsion of oxygen from crystallizing regions or by contamination during annealing.

A pattern similar to the "transformed amorphous" pattern with a broad inner halo has also been observed in thermally evaporated amorphous $Zr_{.40}Cu_{.60}$ but not in sputtered amorphous $Zr_{.40}Cu_{.60}$.[24] This is presumably due to a relatively high level of oxygen contamination in the thermally evaporated sample.

The extent of the conditions under which this (presumably) amorphous ZrO_2-like phase will form is not clear. It had been hoped that such a peak would be seen in our as-prepared or annealed Zr-Cu-O alloys, but the so-far limited studies of these alloys generally produced either an oxygen-stabilized η phase internally or crystalline ZrO_2 phases on the surface. Possibly, higher oxygen contents are necessary in an internal region to produce the amorphous ZrO_2-like phase.

As noted previously, the $Zr_3Cu_3O_x$ phase (η phase, W_3Fe_3C type) was found by X-ray diffraction measurements on the top surface of some melt spun Zr-Cu-O ribbons. However, in other melt spun ribbons of 1, 2 and 4 a/o oxygen, a different, unidentified phase was observed; the reason for this difference is not known. Similar patterns and variability were observed for partly crystalline Zr-Cu-O splats.

Ductility.

It is known that many of the metallic glasses produced by rapid liquid quenching are very ductile, i.e. that they will deform plastically on bending and that foils can even be bent back sharply to form a V-shape without fracturing. This is also true of the binary Zr-Cu, Ti-Ni and Nb-Ni glasses which were prepared in this study. However, it is also known that other amorphous metals do not share this feature and that embrittlement can be caused by annealing, e.g. Ref. 25, while the material appears to remain amorphous. The cause of this brittleness remains a point of controversy.

This study demonstrates clearly that the inclusion of oxygen into the amorphous T-T alloys which were studied enhances brittleness, with increasing O contents causing increasing brittleness. Some amorphous Zr-Cu samples with 2 a/o oxygen were partly brittle; the 4 a/o oxygen alloys were generally partly brittle; amorphous alloys with 6 and 8 a/o oxygen were always brittle, i.e. they would fracture readily on bending with no plastic deformation, and they could not be sheared with scissors. However, it is not yet known if this is an intrinsic property of a homogeneous alloy, i.e. one in which the oxygen is fully dissolved, or whether it is due to the presence of a minute amount of oxygen-induced precipitates; transmission electron microscopy would be required to resolve this point.

Since the ductility of the $Zr_{.49}Cu_{.49}O_{.02}$ alloy varied somewhat from splat to splat, presumably because of a different temperature-time history for each, thermal annealing studies of this alloy were of interest to study this embrittlement. However, this study was hampered by the inability to spin oxygen-containing Zr-Cu alloys to a fully amorphous state to give initially identical samples for annealing studies. Limited studies on splats were therefore made which are thus far inconclusive. Annealing at 700 K for a time corresponding to the first peak in Fig. 2, i.e. corresponding to the formation of a fine-crystalline η phase embedded in the amorphous matrix, produced a very brittle sample; however, annealing for only 5 min at this temperature did not cause embrittlement. Further studies will be necessary to determine whether or not embrittlement can be induced before the fine, oxygen content induced precipitates are apparent to a XRD.

It is noted that a sputtered amorphous Zr-Cu film, nominally 50 a/o Zr, is also very brittle.[26] Whether or not this is due to the presence of gaseous impurities is not yet known.

While no detailed study of the ductility of the Nb-Ni-O glasses was made, the as-prepared glasses were also found to be partly brittle.

Comments on the observation of T_g.

To unambiguously determine whether or not a given amorphous metal displays a glass transition, one must balance the sample size, scanning rate and DSC sensitivity to give a sufficiently large deflection for the ΔC_p. The task of determining ΔC_p is made more complex by the curvature which is generally present in the baseline of the instrument, the "relaxation" which often occurs in the region preceding crystallization, and the need to be sure of the location of the baseline which can shift from run to run due to different thermal configurations of the sample pan and the platinum sample pan cover of the DSC2. For example, the thermogram for the $Zr_{.47}Cu_{.47}O_{.06}$ glass, taken at high sensitivity, qualitatively appears to show a glass transition; however, a careful comparison to the DSC trace for the crystallized material shows that the observed curvature is due primarily to the end of the relaxation effect. Further, any endothermic rise in C_p should be quantized in order to assist in assessing whether or not the "full" ΔC_p is likely to have been observed and thus whether or not the T_g measured from such a trace is in fact accurate.

Because of the high thermal stability of $Nb_{.50}Ni_{.50}$, it could not be determined with the DSC2 whether or not this alloy exhibits a glass transition. However, $Nb_{.40}Ni_{.60}$ was found to exhibit the characteristic relaxation (maximum depth of ~ 1.7 cal/mole K) followed by a rise of ~ 1.1 cal/mole K above the crystalline specific heat, when heated at 80 K/min, although without any indications of a "levelling off". Thus, a glass transition can be seen to begin in amorphous $Nb_{.40}Ni_{.60}$ although the onset of crystallization occurs before the full ΔC_p is achieved.

The sputtered amorphous Zr-Cu behaves similarly[26] to the liquid-quenched $Nb_{.40}Ni_{.60}$. Thus, a relaxation is observed, followed by a ~ 1.3 cal/mole K rise above the crystalline value and then crystallization with a $T_c = 758$ K and $T_p = 769$ K for a 80 K/min scan. (A careful comparison with T_c for a liquid quenched alloy of the same Zr-Cu composition must await an accurate compositional analysis of the sputtered sample.) Since all liquid quenched alloys in this broad compositional region show a well-defined T_g, one might speculate that gaseous impurities in the sputtered film may preclude the observation of the full glass transition. From Fig. 1, it can be seen that about 4 a/o oxygen would produce such behavior in a liquid quenched amorphous $Zr_{.50}Cu_{.50}$.

References

1. M.R. Bennett and J.G. Wright, phys. stat. sol. (a), 1972, 13, 135.
2. P.K. Leung and J.G. Wright, Phil. Mag., 1974, 30, 995.
3. K. Tamura and H. Endo, Phys. Letters, 1969, 29A, 52.
4. H. Matsueda and B.L. Averbach, Mat. Sci. Eng., 1976, 23, 131.
5. H.A. Davies and J.B. Hull, Mat. Sci. Eng., 1976, 23, 193.
6. L.E. Tanner and R. Ray, Scripta Met., 1977, 11, 783.
7. B.C. Giessen, J.C. Barrick and L.E. Tanner, to be published.
8. A.J. Kerns, Ph.D. Thesis, Northeastern University, Boston, Massachusetts. 1974.
9. R.V. Raman, Ph.D. Thesis, Northeastern University, Boston, Massachusetts, 1977.
10. H.S. Chen and D. Turnbull, J. Chem. Phys., 1968, 48, 2560

11. D.E. Polk and H.S. Chen, J. Non-Cryst. Solids, 1974, 15, 165.
12. F. Spaepen and D. Turnbull, in Metallic Glasses, pp. 114-127, 1978, Metals Park, Ohio, ASM.
13. H.S. Chen and E. Coleman, Appl. Phys. Letters, 1976, 28, 245.
14. H.O.K. Kirchner, P. Ramachandrarao and G.A. Chadwick, Phil. Mag., 1972, 25, 1151.
15. Constitution of Binary Alloys, Second Supplement, p. 191, 1969, New York, McGraw Hill.
16. C.B. Shoemaker and D.P. Shoemaker, Acta Cryst., 1967, 23, 231.
17. B.C. Giessen and D. Szymanski, to be published.
18. R.C. Ruhl, B.C. Giessen, M. Cohen and N.J. Grant, Acta Met., 1967, 15, 1693.
19. H.H. Stadelmaier, H. Holleck and F. Thummler, Monatsh. Chemie, 1967, 98, 133.
20. D.E. Polk, A. Calka and B.C. Giessen, Acta Met., 1978, 26, 1097.
21. H.H. Stadelmaier, in Developments in the Structural Chemistry of Alloy Phases, pp. 141-180, 1969, New York, Plenum Press.
22. R.L. Mozzi and B.E. Warren, J. Appl. Cryst., 1969, 2, 164.
23. J.M. Vitek, J.B. Vander Sande and N.J. Grant, Acta Met., 1975, 23, 165.
24. M.Scott, Mater. Sci. Eng., 1977, 30, 219.
25. L.A. Davis, R. Ray, C.-P. Chou and R.C. O'Handley, Scripta Met., 1976, 10, 541.
26. D.E. Polk and C.F. Cline, unpublished results.

Table 1. Thermal Characteristics of Amorphous Samples

Alloy Composition	Heating Rate K/min	T_c^*, K	T_p^*, K	Comments
$Zr_{.50}Cu_{.50}$	80	735	742	T_g^*=681
$(Zr_{.50}Cu_{.50})_{.98}O_{.02}$	80	754+	760	T_g^*=702
$(Zr_{.50}Cu_{.50})_{.96}O_{.04}$	80	764	771	
$(Zr_{.50}Cu_{.50})_{.94}O_{.06}$	80	767	781	
$(Zr_{.50}Cu_{.50})_{.92}O_{.08}$	80	761	771,790	
$Nb_{.50}Ni_{.50}$	10	961	973	
$(Nb_{.50}Ni_{.50})_{.971}O_{.029}$	10	915,956	926,972	
$(Nb_{.50}Ni_{.50})_{.943}O_{.057}$	10	911,956	920,972	
$Nb_{.40}Ni_{.60}$	10	918,∼947,∼964	928,958,981	
"	80	950,∼985	962, –	
∼$Zr_{.50}Cu_{.50}$	80	758	769	sputtered[26]
$Zr_{.50}Cu_{.50}$	10	722.0	726.0	melt spun
"	20	728.5	733.5	"
"	40	736.0	741.0	"
"	80	745.5	750.5	", T_g^*=693
"	160	754.0	760.5	"

* T_g and T_c are defined as the onset temperatures obtained from the intersections of the extrapolated curve preceding crystallization and the steepest tangent to the ΔC_p and the exotherm, respectively. T_p is the temperature at which the crystallization exotherm reaches its maximum.

+ the "shoulder" for this alloy has a T_c=749 K.

crystalline $Zr_{.50}Cu_{.50}$

amorphous $Zr_{.50}Cu_{.50}$

" $(Zr_{50}Cu_{50})_{.98}O_{.02}$

" $(Zr_{50}Cu_{50})_{.96}O_{.04}$

" $(Zr_{50}Cu_{50})_{.94}O_{.06}$

" $(Zr_{50}Cu_{50})_{.92}O_{.08}$

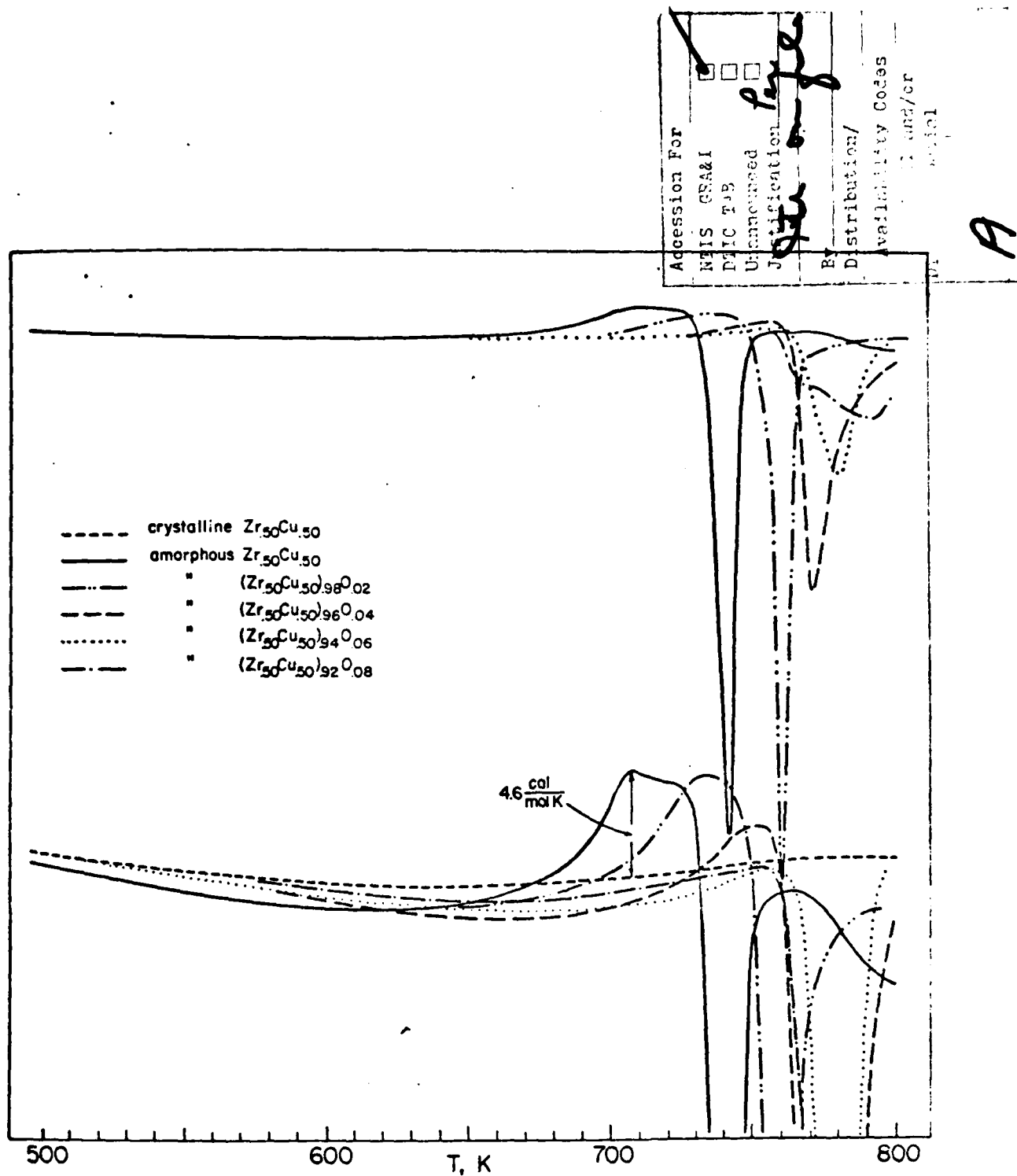$4.6 \dfrac{cal}{mol\,K}$

500   600 700   800

T, K

Figure 1. Thermograms measured with a Perkin Elmer DSC2 at 80 K/min for ~9 mg samples of Zr-Cu-O amorphous metals. The lower set of traces shows the specific heat behavior preceding crystallization; the upper set of traces, recorded at 1/5 of the sensitivity of the lower set, shows the full crystallization exotherm.
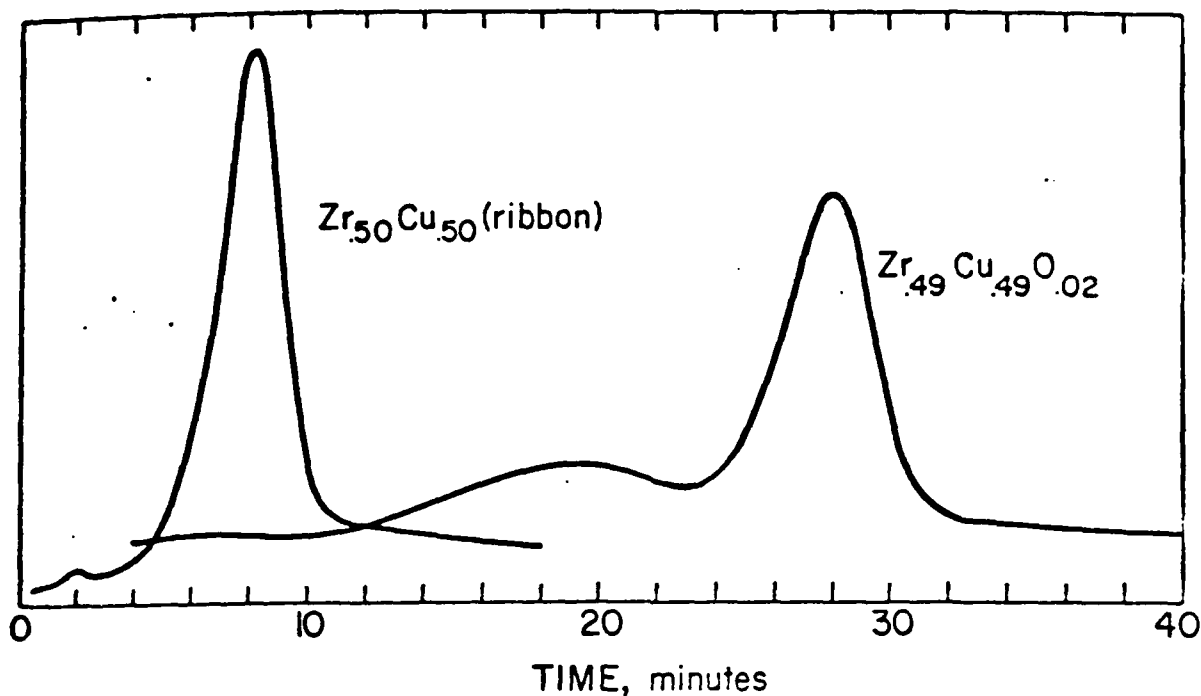
Figure 2. DSC thermograms showing rate of heat evolution as a function of time for indicated samples when annealed at 700 K (displaced zeros). Very small peak at ~2 minutes for the melt spun ribbon is reproducible and may be due to trace amounts of oxygen in this nominally oxygen-free alloy.
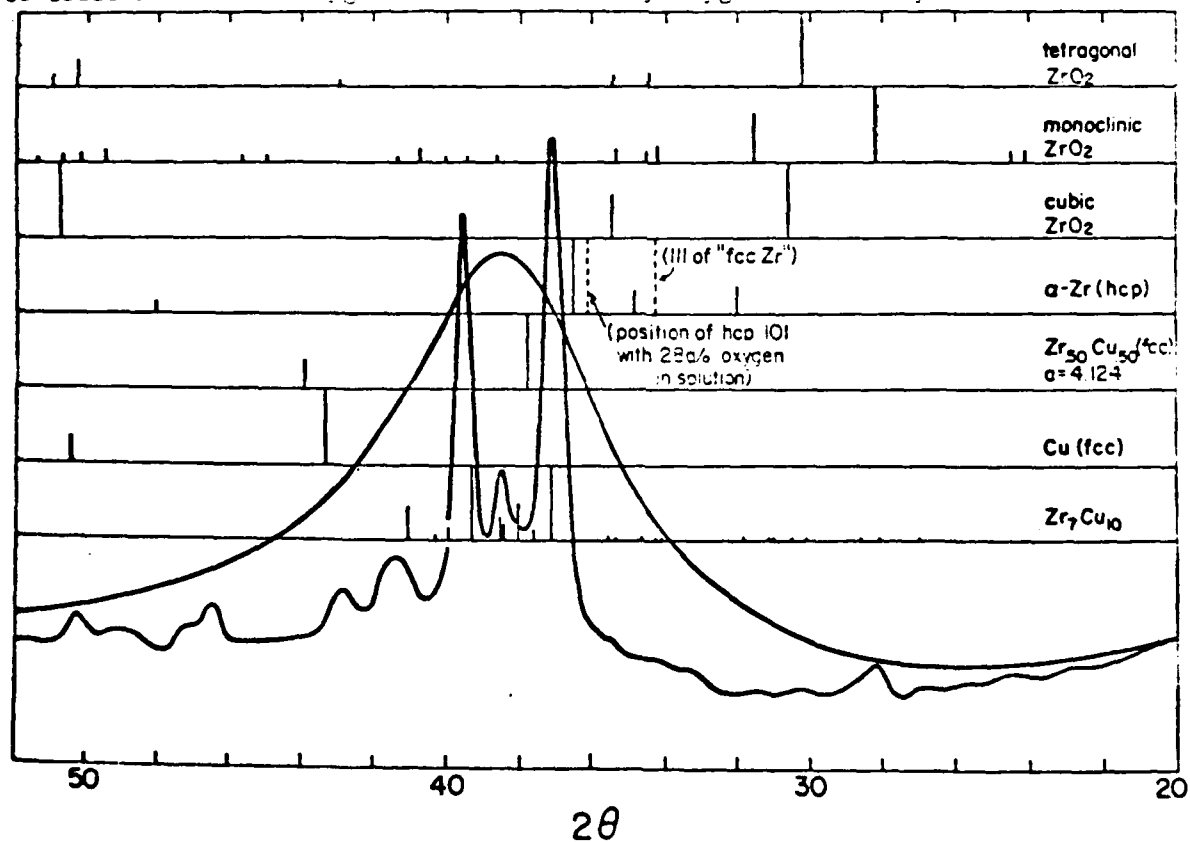

Figure 3. X-Ray diffraction patterns (CuKα radiation) for various phases. The smooth curve is the first broad peak of the pattern obtained from $Zr_{.50}Cu_{.50}$. The crystalline trace is from a crystallized foil of $Zr_{.49}Cu_{.49}O_{.02}$ which contains primarily the α-ZrCu phase.

DATE
ILMED
-8